EELS near-edge structure in the Laves-phase compounds $TiCr_2$ and $TiCo_2$: Theoretical and experimental studies

J. Sun*
School of Materials Science and Engineering, Shanghai Jiao-tong University, Shanghai 200030, People's Republic of China and Center for Solid State Science, Arizona State University, Tempe, Arizona 85287-1704, USA

B. Jiang
Department of Physics and Astronomy, Arizona State University, Tempe, Arizona 85287-1504, USA

David J. Smith
Center for Solid State Science, Department of Physics and Astronomy, Arizona State University, Tempe, Arizona 85287-1704, USA
(Received 28 December 2003; published 23 June 2004)

Laves-phase compounds $TiCr_2$ and $TiCo_2$ have been investigated by electron energy loss spectroscopy (EELS), and *ab initio* calculations have also been performed to relate the experimental spectra based on the method of augmented plane waves plus local orbitals (APW+lo) with the generalized gradient approximation. It is shown that the normalized EELS cross sections of Ti $L_{2,3}$ edges change only slightly between $TiCr_2$ and $TiCo_2$ compounds, and that variations of the calculated valence charge redistributions between these compounds are negligible. Therefore, there are no significant charge transfers between Ti and Cr (Co) atoms, and the local charge neutrality approximation is valid in these compounds. The charge densities of these compounds were also theoretically investigated. The results reveal a relatively strong covalent nature of atomic bonds between Cr–Cr (Co–Co) atoms compared with that between Ti and Cr (Co) atoms in $TiCr_2$ and $TiCo_2$, respectively. It is also demonstrated that the covalent bonding of the atoms in $TiCo_2$ is stronger than that in $TiCr_2$. This result could explain the significant difference of the calculated enthalpies of formation between $TiCr_2$ and $TiCo_2$ compounds.

DOI: 10.1103/PhysRevB.69.214107 PACS number(s): 61.14.−x, 61.50.Lt, 71.20.Lp

I. INTRODUCTION

Laves-phase compounds with the formula AB_2 and topologically close-packed structure are the most abundant class among intermetallic compounds.[1–4] There are three polytypes of structures frequently observed in Laves-phase compounds: namely, cubic C15–$MgCu_2$, hexagonal C14–$MgZn_2$, and dihexagonal C-36 $MgNi_2$ structure. These polytypes have the same basic unit layer, while the stacking sequence of the basic unit layers is different in each structure. The cubic C15 and hexagonal C14 are related in the same way as fcc (*ABCABC* stacking) and hcp (*ABAB* stacking) structures, respectively. The dihexagonal C-36 is basically *ABACABAC* stacking. Although Laves-phase compounds are typical size factor compounds, the stability of these structures is also closely related to the electron concentration,[5,6] impling that the crystal structures are strongly governed by the valence state of the constituent atoms.

Laves-phase compounds have been considered for many important and attractive applications, due to their excellent physical and chemical properties. For example, $CeRu_2$ and $(Hf,Zr)V_2$ have been investigated as superconducting materials,[7,8] and $(Tb,Dy)Fe_2$ as giant magnetostrictive materials.[9,10] $ZrCr_2$ and $TiMn_2$ exhibit favorable hydriding–dehydriding kinetics and large hydrogen-absorbing capability as hydrogen storage materials.[11,12] Because of the high melting point, high strength at elevated temperatures and reasonably good oxidation resistance, $NbCr_2$, $TiCr_2$, and HfV_2 have been studied recently for high-temperature structural applications.[13–15] In order to further understand the physical and chemical properties of these compound materials, therefore, an investigation of the electronic structure and bonding characteristic of Laves-phase compounds has both fundamental scientific and technological significance.

Some understanding of bonding characteristics in intermetallic compounds can be deduced from their thermodynamic properties. Generally speaking, the low magnitude of the exothermic enthalpy of formation corresponds to metallic bonding, whereas the high magnitude of the exothermic enthalpy of formation relates to covalent and ionic bonding. Robinson *et al.*[16] related the values of enthalpies of formation of intermetallic compounds to bonding characteristics. The enthalpies of formation for most covalent intermetallics were found to range approximately from −40 to −100 kJ/mol. The bonding nature in Laves phases is generally considered to be metallic because their enthalpies of formation are low.[16] Recently, Liu *et al.*[17] surveyed the enthalpies of formation in transition-metal Laves-phase compounds. They found that when the atomic number increases for the later transition metal, the enthalpies of formation increase in the order of $V \rightarrow Cr \rightarrow Mn \rightarrow Fe \rightarrow Co \rightarrow Ni$, with a wide range from several kJ/mol to several hundred kJ/mol, for Laves phases formed between early transition metals and these elements. It was speculated that bonding characteristics in Laves phases are complicated, and that metallic, covalent, and ionic bonds might be present in these compounds. *Ab initio* calculations of charge density in the C15 HfV_2 and

$NbCr_2$ showed that the bonding is only weakly directional.[18] A recent charge density study of $MgCu_2$ by the maximum entropy method demonstrated that strong covalent bonding exists between the Cu–Cu atoms, while electrons are distributed similarly to metallic bonding between Mg and Cu atoms.[19]

Electron energy loss spectroscopy (EELS) is an important experimental technique to study the electronic structure of materials.[20–22] Electron energy loss near edge structure (ELNES) provides information on the actual density of states (DOS) distribution above the Fermi level. Botton *et al.*[23] and Muller *et al.*[24] observed an obvious change of ELNES upon the formation of transition-metal aluminides, such as NiAl, Ni_3Al, FeAl, and CoAl, and the changes of ELNES were successfully reproduced by augmented-plane-wave calculations. These results revealed the bonding trends between the Al and transition-metal atoms. Potapov *et al.*[25] recently performed an ELNES study of some Ni-based intermetallic compounds. They found that the formation of intermetallic compounds between Ni and other transition metals resulted in measurable changes in the ELNES of the Ni $L_{2,3}$ ionization edge, and the observed changes were interpreted in terms of hybridization between the Ni *d* and the transition metal *d* bands.

The purpose of this paper is to explore the bonding characteristic of the transition-metal Laves-phase compounds. Two types of C15 Laves-phase compounds, including $TiCr_2$ and $TiCo_2$, have been investigated comparatively. The enthalpies of formation of $TiCr_2$ and $TiCo_2$ are supposed to be different, which may result from different bonding characteristics between these compounds. Excitations of the 2*p* subshell in $TiCr_2$ and $TiCo_2$ have been studied by inelastic scattering of 100-keV electrons. The Ti, Cr, and Co $L_{2,3}$ white lines, which arise from the dipole transition to unoccupied *d* states, and in particular the Ti $L_{2,3}$ edge difference between $TiCr_2$ and $TiCo_2$ compounds, have been investigated in terms of their shapes and integral cross sections, which are related to the *d*-band occupancy. *Ab initio* calculations have been conducted to relate the experimental spectra based on the method of augmented plane waves plus local orbitals (APW+lo) with the generalized gradient approximation (GGA). The enthalpies of formation for $TiCr_2$ and $TiCo_2$ compounds have been obtained by calculating the total energy. The charge density distributions in these compounds were also theoretically investigated in the present work.

This paper is organized as follows. In Sec. II, we describe the details of *ab initio* calculations based on the APW+lo method, materials preparations and measurements, and processing of the EELS spectra. Results of EELS measurements and *ab initio* calculations by APW+lo are presented in Sec. III. Based on these results, the bonding characteristics of $TiCr_2$ and $TiCo_2$ compounds are investigated in this section. Conclusions are finally drawn in Sec. IV.

II. METHODS

A. Theoretical calculations

Ab initio calculations of the electronic structure and total energy of the $TiCr_2$ and TiCo2 Laves-phase compounds were performed using the method of augmented plane wave plus local orbitals, as implemented in the software package WIEN2K,[26] where the core states are treated fully relativistically, and the semicore and valence states are treated within a scalar relativistic approximation. The main advantage of the APW+lo method is that it converges faster and reaches the same accuracy as the linearized augmented-plane-wave method. Inside the atomic spheres, the potential and charge densities are expanded in lattice harmonics up to $L=10$. Exchange and correlation effects are treated within density functional theory, using the generalized gradient approximation.[27] The same muffin-tin radius (R_{mt}) of 2.3 a.u. was chosen for Ti in the different compounds, and 2.2 a.u. for Cr and Co atoms. A plane-wave cutoff ($R_{mt}K_{\max}$) of 9.0 was used. The calculations were performed with a 2400 κ-point mesh, yielding 84 κ points in the irreducible wedge of the Brillouin zone for the C15 structure. Convergence was assumed when the energy difference was less than 0.1 mRy. The Brillouin zone integration was carried out according to a modified tetrahedron method.[28] The theoretical lattice constant calculated by this method is only 0.9% smaller than the experimental lattice constant for the Laves-phase compound,[29] so experimental lattice constants of 6.932 Å for $TiCr_2$ and 6.692 Å for $TiCo_2$ were used in our calculations.[30,31]

ELNES simulations were performed by calculation of the differential cross section using the Fermi golden rule.[32] For small-angle scattering, the dipole approximation is applied. Thus, the EELS intensity can be written as the product of a DOS and an atomic transition matrix[33]

$$I(E,\mathbf{q}) \propto |\langle f|\mathbf{q}\cdot\mathbf{r}|i\rangle|^2\rho(E) \propto |\mathbf{q}\cdot\langle f|\mathbf{r}|i\rangle|^2\rho(E),$$

where $|i\rangle$ and $|f\rangle$ represent the initial and final states of the excited electron, respectively, $\rho(E)$ is the unoccupied DOS, and $\mathbf{q}$ is the momentum transfer. Here, the ELNES spectra were calculated by combining the computed DOS with the matrix elements for the transition from the initial to final states. This method is based on the single particle approximation, which assumes that final states are not modified significantly by *d* electron exchange and core hole effects. However, the excitation process causes an intensity redistribution, and the core hole and exchange interactions are important when the screening effects are not effective,[34] which might result in difficulties in comparison of theory with experiment for the $L_{2,3}$ transition $2p^6 \rightarrow 2p^5 3d^{n+1}$.

B. Materials and experimental details

Two different types of C15 Laves-phase compounds, including $TiCr_2$ and $TiCo_2$, were investigated in the present work. Small button ingots with weight of 60 g were prepared by arc-melting on a water-sealed copper hearth in an argon atmosphere. The button ingots were remelted several times to ensure chemical homogeneity. The ingots were annealed in vacuum at 1525 K for 48 h, and then cooled to room temperature within the furnace. The ingots were crushed into fine powders. Electron microscopy specimens were prepared by picking up tiny pieces of powders of $TiCr_2$ and $TiCo_2$ crystals suspended in isopropanol using a holy carbon film across a copper grid.

Electron energy loss spectra were collected using a parallel recording Gatan 666 spectrometer fitted to a Philips EM400 equipped with a field-emission gun operating at 100 keV. The $L_{2,3}$ edges were acquired in the diffraction mode. The energy resolution of the spectrometer is typically around 1.0 eV, measured as the full width at half maximum at the zero-loss peak. The spectra were corrected for the detector dark current and gain variation by averaging several spectra acquired at different positions on the photodiode array. The continuum background was fitted and subtracted at pre-edge intensities using a standard exponential procedure. Spectra were also deconvoluted using the Fourier-ratio method,[35] as the low loss contribution from the same area measured separately. Oxygen *K* edges were detected in some spectra, but the offset of the O *K* edge is negligibly low, indicating that the films were reasonably pure.

III. RESULTS AND DISCUSSION

The background subtracted and low loss deconvoluted Ti, Cr, and Co $L_{2,3}$ edges in $TiCr_2$ and $TiCo_2$ Laves-phase compounds are shown in Fig. 1. The peaks of the spectrum of $TiCr_2$ are slightly higher and wider than those of $TiCo_2$, but the general features of Ti $L_{2,3}$ edges look similar for these compounds. The ratio between the L_3 $(2p_{1/2} \rightarrow d_{3/2})$ and L_2 $(2p_{3/2} \rightarrow d_{3/2,5/2})$ white line integrated intensities was estimated to be 0.76, 1.3, and 3.1 for Ti, Cr, and Co, respectively. The results are consistent with those obtained from pure metals and some intermetallic compounds (0.7–0.75 for Ti and 1.2 for Cr).[36,25] On the basis of the $2j+1$ degeneracy of the initial $2p_{1/2}$ and $2p_{3/2}$ core states, the ratio of L_3 to L_2 intensity is expected to be 2:1. The observed anomalous ratio possibly arises from the exchange interaction of *d* electrons.[34,36]

Based on the assumption that the cross section for the $L_{2,3}$ edge of an atom is always asymptotic to the same value, regardless of the atomic environment,[37] the spectra obtained were normalized using the method proposed by Pearson *et al.*[38,39] This makes it possible to quantitatively analyze the changes of ELNES acquired from different materials. Here, the normalized window of 10 eV in width began at 20 eV after the L_2 onset. All cross sections were then divided by this normalized window. Furthermore, an atomic-like term, corresponding to scattering from the core shell of a free atom to the free-electron continuum modeled by the Hartree–Slater function, was obtained from Rez calculation[40] for each element and added in Fig. 1. Thus, the cross section isolated from the theoretical atomic-like one represents a measurement of the number of holes in the *d* bands. A similar normalization method was used for measurements of the number of *d* holes in both pure metals and Ni-based intermetallic compounds.[38,39,24,25] The normalized cross sections integrated over an energy window from the L_3 onset (L_3-3) to L_2+20 eV are given in Table I. The normalized cross sections, which represent the measured number of *d* holes, decrease in the order of $Ti \rightarrow Cr \rightarrow Co$, which is qualitatively consistent with the results for pure metals and some Ni-based intermetallic compounds.[39,25] The number of *d* holes around Ti atoms is only slightly higher in the $TiCr_2$ than that in the $TiCo_2$ compound.

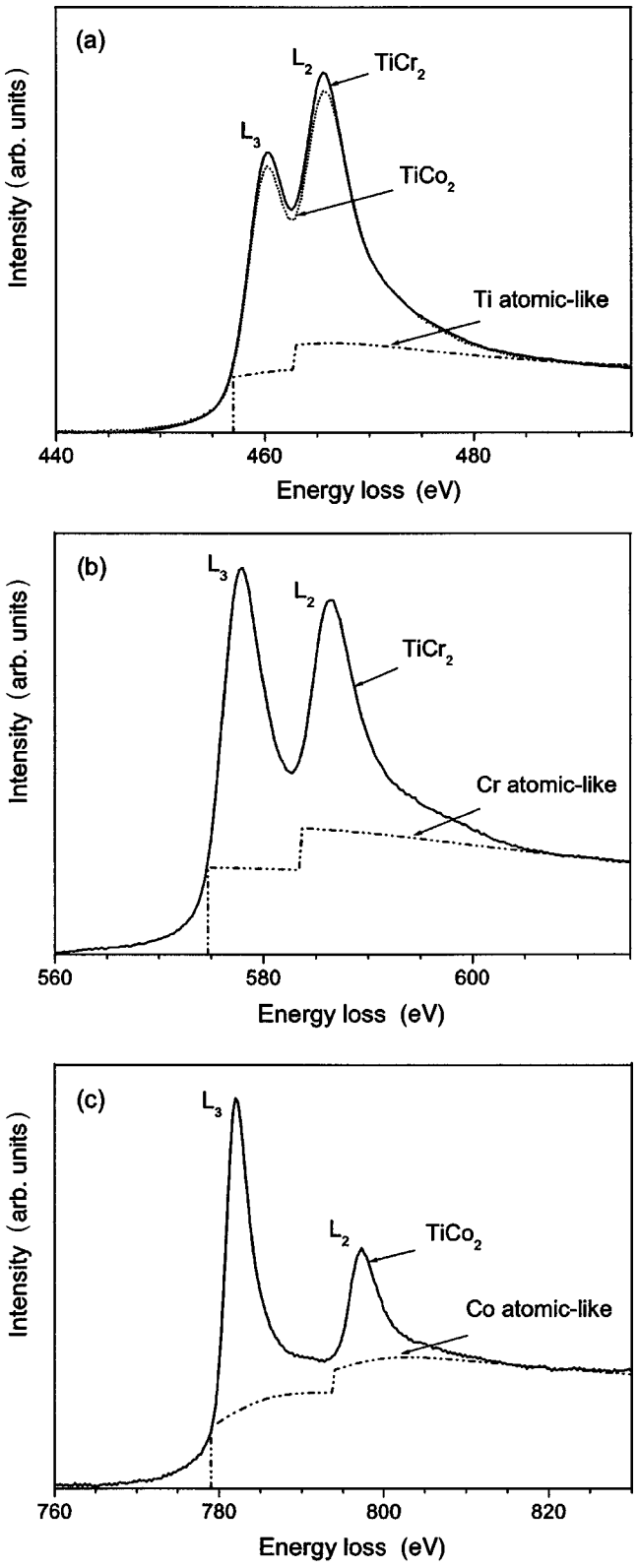

FIG. 1. Measured $L_{2,3}$ ionization edges for Ti (a), Cr (b), and Co (c) in the $TiCr_2$ and $TiCo_2$ compounds. The calculated atomic-like cross sections are also plotted for these atoms. The spectra are scaled by the atomic-like cross sections.

TABLE I. Ti, Cr, and Co, $L_{2,3}$ normalized cross sections for $TiCr_2$ and $TiCr_2$ compounds. I_1 is the normalized cross section and I_2 the normalized cross sections subtracted by the atomic-like section calculated by Rez (Ref. 40).

Ionization edge	Compound	I_1	I_2
Ti $L_{2,3}$ edge	Ti atomic-like	3.058	
	$TiCr_2$	6.892	3.834
	$TiCo_2$	6.752	3.694
Cr $L_{2,3}$ edge	Cr atomic-like	3.312	
	$TiCr_2$	6.403	3.091
Co $L_{2,3}$ edge	Co atomic-like	3.287	
	$TiCo_2$	5.242	1.955

Figure 2 shows the calculated total densities of states for $TiCr_2$ and $TiCo_2$ compounds. The calculated partial densities of states for these compounds are shown in Fig. 3. As a reference, the total and partial DOS for pure Ti metal are also calculated and plotted in these figures. The total DOS are formed mainly by the *d* states. The dominant contribution to DOS near the Fermi level and at lower energies comes from the *d* states of Cr and Co, while DOS at high energies are dominated by the *d* states of Ti in $TiCr_2$ and $TiCo_2$. The DOS profile shows a deep valley separating the low-energy bonding and high-energy antibonding regions for $TiCr_2$ compound. For $TiCo_2$, there are well-defined peaks associated with the bonding and nonbonding regions of Co and Ti, with the Ti nonbonding states fully unoccupied. The most important feature of these DOS is the overlapping of 3*d* states from Ti and 3*d* states from Cr (Co) in the construction of $TiCr_2$ ($TiCo_2$) electronic energy bands, which implies hybridization between the Ti *d* and Cr (Co) *d* states on formation of $TiCr_2$ ($TiCo_2$) compounds. A further analysis of the decomposed *d* DOS showed the bonding between the Ti and Cr (Co) atoms is mainly contributed by hybridization between the $d_{t_{2g}}$ orbital on the Ti sites and the orbital made up of $d_{x^2-y^2}$ and d_{xy} on the Cr (Co) sites.

The valence charges, which are partitioned by the site and angular momentum, were calculated for pure Ti metal and the $TiCr_2$ and $TiCo_2$ compounds, and results are given in Table II. The data calculated by Potapov *et al.*[25] for the TiNi compound with *B*2 structure are also included for a reference. The same muffin-tin radius of 2.3 a.u. was adopted for Ti atom in the pure Ti and the $TiCr_2$ and $TiCo_2$ compounds since total charge is sensitive to the chosen sphere size. As seen from Table II, the number of *d* electrons in the Ti muffin-tin sphere is almost the same between $TiCr_2$ and $TiCo_2$ compounds, and also very close to that of the TiNi intermetallic compound. (Although the number of *d* electrons slightly increases from $TiCr_2$ to TiNi, the differences of $\sim$0.03 electron/atom between these compounds are negligibly small.) The valence charge redistribution of Ti atoms in the muffin-tin sphere on formation of $TiCr_2$ and $TiCo_2$ compounds is very small compared with pure Ti metal.

The theoretical Ti L_3 ($L2$) spectra have been calculated according to the equation described in Sec. II. In order to compare the theoretical and experimental spectra, it is necessary to account for instrumental broadening of the spectrometer. This energy resolution function is approximated by a Lorentzian function about 1.0 eV in width for the Ti $L_{2,3}$ edge. The calculated Ti L_3 ($L2$) edges in $TiCr_2$ and $TiCo_2$ compounds are shown in Fig. 4. The peak for Ti L_3 ($L2$) spectrum of $TiCr_2$ is slightly higher than that of $TiCo_2$, but the general shapes of Ti L_3 ($L2$) spectra for these compounds are similar, which is consistent with the experimental results. It should be noted that our calculation of the ELNES is performed based on the single particle approximation, assuming that final states are not modified significantly by *d*-electron

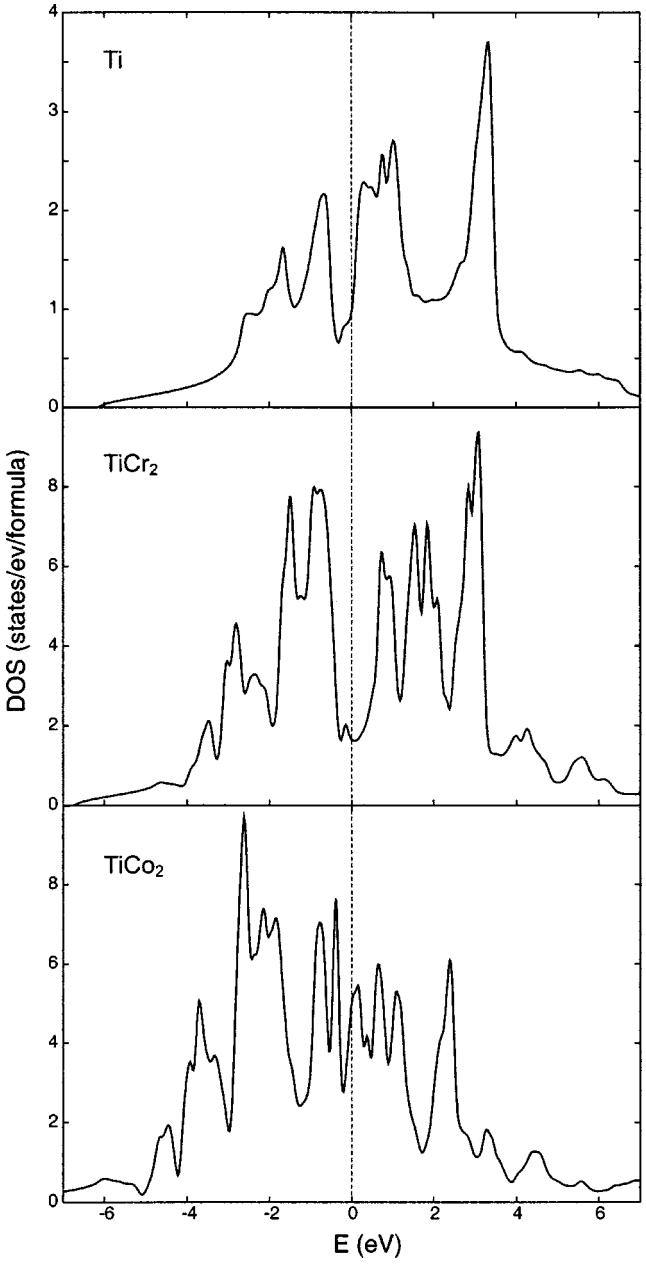

FIG. 2. APW+lo calculated total densities of states for pure Ti metal and the $TiCr_2$ and $TiCo_2$ compounds. The Fermi energy is taken as the zero of the energy axis.

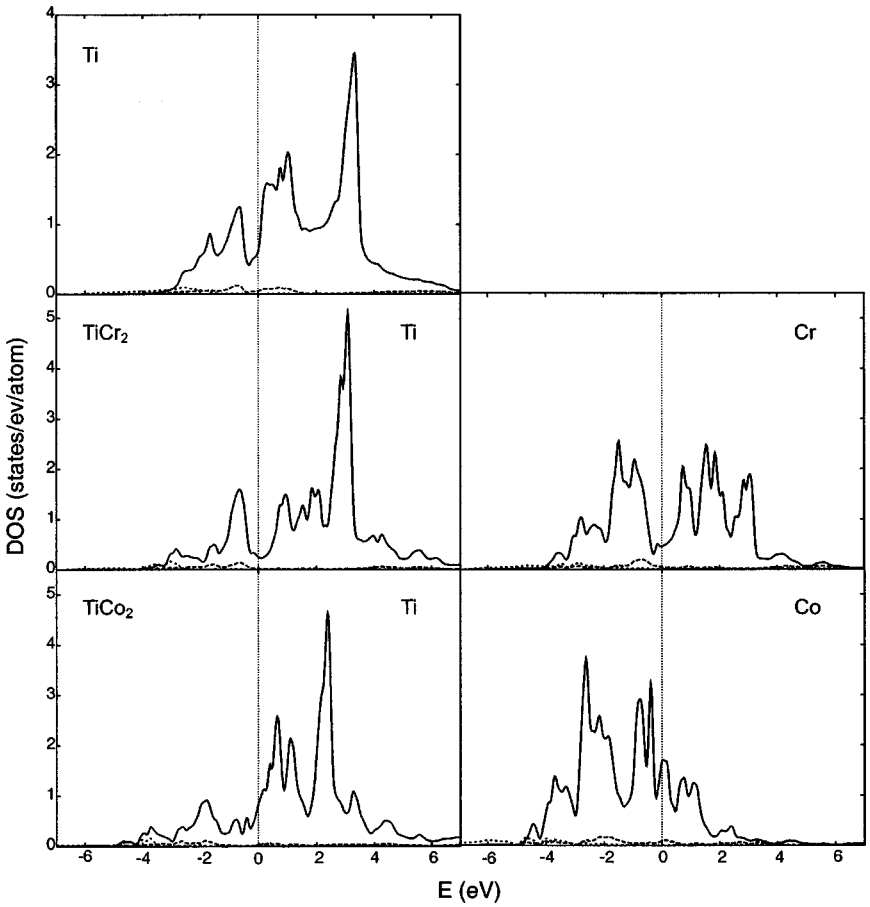

FIG. 3. APW+lo calculated partial densities of states (*s*—dot line, *p*—dash line, and *d*—solid line) for pure Ti metal and the $TiCr_2$ and $TiCo_2$ compounds.

exchange and core hole effects. Theoretical simulations of the Ti $L_{2,3}$ edges cannot predict the anomalous ratio between the L_3 and L_2 white line integrated intensities observed in $TiCr_2$ and $TiCo_2$ compounds. Similar results were also found for the Ti $L_{2,3}$ edges in TiAl intermetallic compound by Botton *et al.*[41] These discrepancies between the theory and experiment arise from the many-body effects under the influence of the core hole in the 2_p state, which introduces redistributions of the DOS because the *d* bands in Ti atoms are nearly empty and cannot screen the core hole successfully. A dynamic-screening calculation is therefore necessary to solve this problem.[42]

Earlier work performed by Potapov *et al.*[25] showed that the formation of intermetallic compounds between Ni metal and Al and other transition metals causes a measurable variation in the ELNES of the Ni $L_{2,3}$ ionization edge of those compounds. The present results show that only a small variation in Ti $L_{2,3}$ ionization edges was detected between the two different types of $TiCr_2$ and $TiCo_2$ compounds, both theoretically and experimentally. This can be explained by hybridization between the Ti *d* and Cr (Co) *d* states on formation of $TiCr_2$ ($TiCo_2$) compounds. As seen from Fig. 3, there are high densities of unoccupied states spreading far above the Fermi level for *d* states. The unoccupied states are fewer and nearer the Fermi level for the Co *d* states compared with those for the Cr *d* states. Ti–Cr (–Co) hybridizations result in a slight shift of empty states to the Fermi level for the Ti *d* states upon formation of $TiCr_2$, more so upon formation of $TiCo_2$ compounds.

EELS studies of a series of 3*d* and 4*d* transition metals have shown that the white line intensity decreases approximately linearly with the occupancy of the *d* state in each

TABLE II. The calculated valence charges in the muffin-tin spheres and the interstitial regions for pure Ti metal and the $TiCr_2$ and $TiCo_2$ compounds, expressed in electron/atom. The values of the TiNi compound with *B*2 structure calculated by Potapov *et al.* (Ref. 25) are also listed. M represents Cr, Co and Ni in the different compounds, respectively.

	Ti *s*	Ti *p*	Ti *d*	Ti *f*	M *s*	M *p*	M *d*	M *f*	Interstitial
Ti	0.231	0.195	1.804	0.007					1.748
$TiCr_2$	0.209	0.238	1.726	0.010	0.314	0.292	3.855	0.017	1.600
$TiCo_2$	0.207	0.225	1.753	0.016	0.414	0.387	7.044	0.022	1.313
TiNi	0.224	0.237	1.773	0.021	0.518	0.394	8.243	0.012	1.289

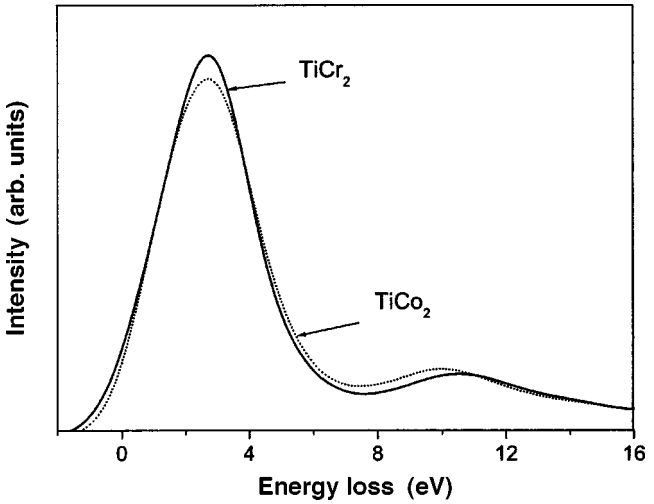

FIG. 4. The calculated Ti L_3 (L_2) ELNES for $TiCr_2$ and $TiCo_2$ compounds, respectively.

series.[38] The changes in the white line intensities were also interpreted as charge transfers upon alloying of copper with other transition metals.[39] Recently, Muller *et al.*[24] accurately measured the Ni $L_{2,3}$ cross sections in Ni–Al system, including Ni, Ni_3Al, and NiAl. Their measurements revealed no significant changes in the number of *d* holes around Ni atoms among pure Ni metal, Ni_3Al, and NiAl compounds. Furthermore, an experimental study of Ni $L_{2,3}$ edges in some nickel-based transition-metal compounds showed that changes in the number of *d* holes around Ni atoms are also negligibly small.[25] They argued that the total number of charges around each atom does not change significantly, and local charge neutrality is valid upon formation of compounds. The pronounced changes of the ELNES can be interpreted by hybridization (i.e., covalence) between Ni and Al (other transition-metal) atoms, which clearly reflects the bonding nature of atoms in those intermetallic compounds. In this work, the difference of measured *d* holes around Ti atoms between the $TiCr_2$ and $TiCo_2$ compounds is negligible. The theoretical calculation also showed a very small variation of the valence charge redistribution in the Ti muffin-tin sphere among pure Ti metal and the $TiCr_2$ and $TiCo_2$ compounds. Therefore, it can be concluded that there are no significant charge transfers upon formation of $TiCr_2$ and $TiCo_2$ compounds, and the local charge neutrality approximation is effective in these Laves-phase compounds.

The enthalpies of formation for $TiCr_2$ and $TiCo_2$ were calculated in the present work. In order to obtain the enthalpies of formation of $TiCr_2$ and $TiCo_2$, the total energies of pure Ti, Cr, and Co metals were also calculated using their experimental lattice constants, respectively. The ground state of Co is ferromagnetic, so spin-polarized calculations were performed for Co. However, $TiCo_2$ was found to be nonmagnetic. The enthalpy of formation is defined as the total energy difference between the compound and the constituents in proportion to composition. Results are given in Table III. The calculated enthalpy of formation for $TiCr_2$ is comparable with the theoretical value of -0.10 eV/atom for $ZrCr_2$.[29] The enthalpy of formation is in a good agreement with the experimental value of -0.35 eV/atom for $TiCo_2$.[17] These enthalpies of formation for $TiCr_2$ and $TiCo_2$ are close to those for the covalent intermetallic compounds as indicted by Robinson *et al.*[16] It is also noted that the enthalpy of formation for $TiCo_2$ is significantly larger than that for $TiCr_2$. This implies that the bonding characteristic is possibly different between the $TiCr_2$ and $TiCo_2$ compounds.

TABLE III. The calculated enthalpies of formation for the $TiCr_2$ and $TiCr_2$ compounds.

Compounds	Enthalpies of Formation (ev/atom)
$TiCr_2$	-0.13
$TiCo_2$	-0.31

In order to further explore the bonding characteristics in $TiCr_2$ and $TiCo_2$ compounds, charge densities in $TiCr_2$ and $TiCo_2$ were theoretically calculated. Charge density distribution maps on the $(1\bar{1}0)$ plane for $TiCr_2$ and $TiCo_2$ are shown in Fig. 5, which provide further information about bonding characteristics for these compounds. The contour lines are plotted from 0.0 to 0.6 $e/Å^3$ with 0.03-$e/Å^3$ intervals, and

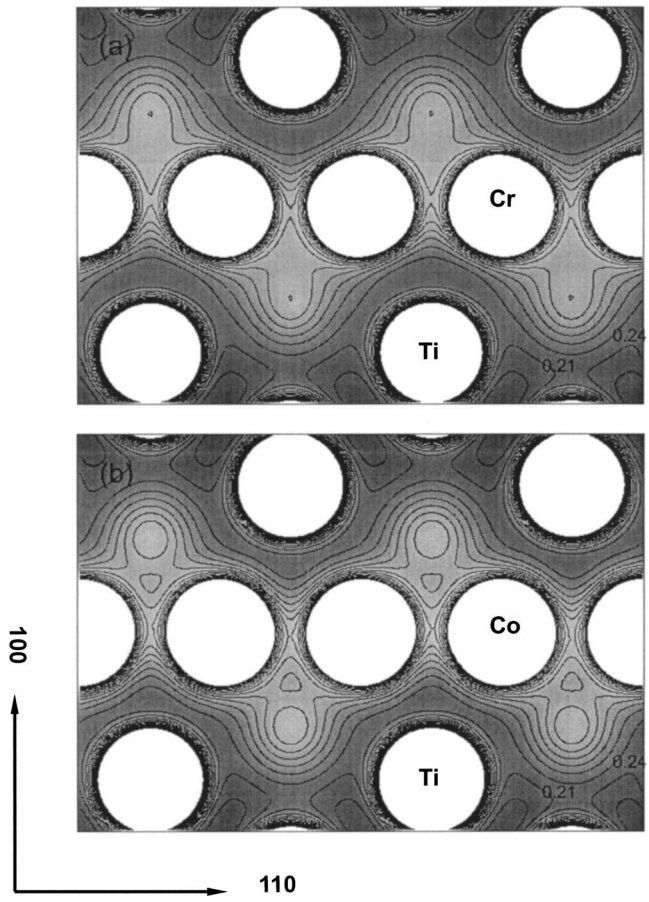

FIG. 5. The charge density contour plots on the $(1\bar{1}0)$ plane of $TiCr_2$ (a) and $TiCo_2$ (b) compounds. The contour lines are plotted from 0.0 to 0.6 $e/Å^3$ with 0.03-$e/Å^3$ intervals.

contour lines of high charge density are omitted. In the C15 structure of $TiCr_2$ and $TiCo_2$, Ti atoms occupy the diamond-type lattices and Cr or Co atoms are located at tetrahedral sites. The $(1\bar{1}0)$ plane bisects the Cr (Co) tetrahedral in $TiCr_2$ and $TiCo_2$. Figure 5 shows that Ti atoms are almost spherical in $TiCr_2$ and $TiCo_2$, but the contour line of low charge density around Ti atoms, for example 0.24 $e/Å^3$, moves obviously towards Cr (Co) atoms, respectively. In contrast, Cr and Co atoms are anisotropic. These results clearly indicate the directional *d* bonding in $TiCr_2$ and $TiCo_2$, which is consistent with the results of the DOS analysis described above. The observed overlap of electron densities between Cr–Cr atoms implies a covalent bonding between Cr–Cr atoms due to hybridization of the *d* orbitals in $TiCr_2$, as shown in Fig. 5(a). The height of the charge density at the bond midpoint between Cr–Cr atoms was found to be 0.391 $e/Å^3$, whereas the height of the charge density at the bond midpoint between Ti and Cr atoms is only 0.230 $e/Å^3$. It could be assumed that the Ti–Cr hybridization is weaker compared with the Cr–Cr in the $TiCr_2$ compound. This can be understood through the C15 crystal structure of the Laves-phase compound. In the $TiCr_2$ structure, 6 Cr atoms occupy the nearest neighboring sites of Cr. The atomic distance between the nearest Cr–Cr atoms is 4.632 a.u. This value is shorter by 2.7% than that of 4.762 a.u. in pure Cr metal with bcc structure. The atomic distance between the next nearest Ti–Cr atoms is 5.431 a.u. The Cr–Cr hybridization is therefore stronger than the Ti–Cr hybridization in $TiCr_2$, and even stronger than the Cr–Cr hybridization in the bcc Cr metal. (The height of the charge density at the bond midpoint between the Cr–Cr atoms was calculated to be 0.348 $e/Å^3$ in the bcc Cr metal.)

The same phenomenon was observed for the $TiCo_2$ compound shown in Fig. 5(b). The height of the charge density at the bond midpoint between Co–Co atoms is 0.420 $e/Å^3$, whereas this value is only 0.233 $e/Å^3$ between Ti–Co atoms in $TiCo_2$. Similarly, 6 Co atoms occupy the nearest neighboring sites of Co in the $TiCo_2$ structure. The atomic distance between the nearest Co–Co atoms is 4.471 a.u., which is shorter by 5.2% than that of 4.718 a.u. in pure Co metal with hcp structure, while the atomic distance between the next nearest Ti–Co atoms is 5.243 a.u. Thus, the Co–Co hybridization is stronger than the Ti–Co in $TiCo_2$, and stronger than the Co–Co hybridization in the hcp Co metal. (The height of the charge density at the bond midpoint between Co–Co atoms was found to be 0.335 $e/Å^3$ in the hcp Co metal.) The heights of the charge density at the bond midpoint between atoms in $TiCo_2$ are higher than those in $TiCr_2$, in particular compared to those between Co–Co atoms and Cr–Cr atoms. It could be said that there is a stronger covalent bonding in the $TiCo_2$ than in the $TiCr_2$ compound. It is also worth noting that the hybridization between Cr–Cr (Co–Co) atoms is stronger in these Laves-phase compounds compared with those in pure Cr (Co) metals, especially between Co–Co atoms, due to reduction of the atomic distances in these compounds. The contribution to enthalpies of formation comes not only from the Ti–Cr (Co) hybridization, but also from the relatively strong Cr–Cr (Co–Co) hybridization upon formation of $TiCr_2$ and $TiCo_2$ compounds. The difference of enthalpies of formation between the $TiCr_2$ and $TiCo_2$ compounds could be explained by the different degree of covalent bonds existing in these compounds. The stronger covalent bonding between atoms, in particular between Co–Co atoms, seems to correspond to the higher magnitude of enthalpy of formation in the $TiCo_2$ compound.

Ormeci *et al.*[18] calculated the charge densities in C15 HfV_2 and $NbCr_2$ compounds based on a full potential muffin-tin orbital method. Their results showed that the bonding is only weakly directional for these compounds. Our calculated results for $TiCr_2$ and $TiCo_2$ compounds are comparable with the height of the charge densities at the bond midpoint of 0.51 $e/Å^3$ for Cu–Cu atoms in $MgCu_2$ obtained by Kubota *et al.*[19] using the maximum entropy method. They argued that hybridization between Cu atoms is very significant due to the high value of the charge density of the interatomic region. (This value is 0.61 $e/Å^3$ for a typical covalent crystal, such as Si.[43]) The height of the charge densities in the interatomic region of Mg and Cu is only 0.19 $e/Å^3$, and electron distribution resembles metallic bonding between Mg and Cu atoms. The strong Cu–Cu bonding along the Kagome net[44] forms a tetrahedral electronic network in the $MgCu_2$ structure. Hirata *et al.*[45] recently reported a significant evidence for the covalent bonding in the C15 $TiCr_2$ Laves-phase compound. The observed icosahedral clusters in the C15 $TiCr_2$ are ascribed to the formation of local covalent bonds between Cr atoms, and the development of a three-dimensional network of covalent tetrahedra of Cr atoms causes phase transformation of the C15 structure from the bcc structure. Their experimental observations are consistent with the present calculations of charge densities, which exhibit a relatively strong covalent nature of atomic bonds between Cr–Cr atoms in $TiCr_2$. These covalent bonds result in a tetrahedral network of Cr atoms in the $TiCr_2$ compound.

IV. CONCLUSIONS

It has been demonstrated that electron energy loss spectroscopy and *ab initio* APW+lo calculation provide a significant technique to study the electronic structure or bonding characteristic in materials. In the case of C15 Laves-phase compounds $TiCr_2$ and $TiCo_2$, a small variation in Ti $L_{2,3}$ ionization edges was measured between these compounds. These variations can be interpreted in terms of hybridization between the Ti *d* and Cr (Co) *d* states from the decomposed densities of states. The accurate measurement of the normalized EELS cross sections showed that there are no significant changes of the number of *d* holes around Ti atoms between $TiCr_2$ and $TiCo_2$ compounds. The theoretical calculation also showed negligible variations of the valence charge redistribution in the Ti muffin-tin sphere for pure Ti metal, $TiCr_2$, and $TiCo_2$; local charge neutrality approximation is thus valid in these compounds.

Total energy calculations show that the enthalpy of formation for $TiCo_2$ is significantly larger than that for $TiCr_2$, which implies different bonding characteristics between $TiCr_2$ and $TiCo_2$. The charge density distributions in these compounds were therefore investigated theoretically. The results reveal a relatively strong covalent nature of atomic

bonds between Cr–Cr (Co–Co) atoms compared with that between Ti and Cr (Co) atoms in $TiCr_2$ and $TiCo_2$, respectively. From measurement of the heights of the charge density at the bond midpoint between atoms, it can be concluded that the covalent bonding in $TiCo_2$ is stronger than that in $TiCr_2$. The difference of enthalpies of formation between $TiCr_2$ and $TiCo_2$ could be interpreted in terms of the different degree of covalent bonds existing in these compounds.

ACKNOWLEDGMENTS

This research was sponsored by the National Natural Science foundation of China (Project Number 50271040). B. Jiang acknowledges support from DOE DE-FG03-02ER45596. The authors thank Professor Peter Rez (ASU) for many helpful discussions. The use of facilities in the John M. Cowley Center for High Resolution Electron Microscopy at Arizona State University is also acknowledged.

*Electronic address: jsun@sjtu.edu.cn

[1] F. Laves, *Theory of Alloy Phase* (American Society for Metals, Metals Park, OH, 1956).
[2] J. H. Wernick, in *Intermetallic Compound*, edited by J. H. Westbrook (Wiley, New York, 1967), p. 197.
[3] A. K. Sinha, Prog. Mater. Sci. **15**, 79 (1972).
[4] T. B. Massalski, in *Physical Metallurgy*, edited by R. W. Cahn and P. Hassen (North-Holland, New York, 1983), Part 1, p. 190.
[5] F. Laves and H. Witte, Metallwirschaft **15**, 840 (1936).
[6] Y. Komura and Y. Kitano, Acta Crystallogr., Sect. B: Struct. Crystallogr. Cryst. Chem. **33**, 2496 (1977).
[7] K. Inoue and K. Tachikawa, IEEE Trans. Magn. **15**, 635 (1979).
[8] Z. Wu, N. L. Saini, S. Agrestini, D. D. Castro, A. Bianconi, A. Marcelli, M. Battisti, D. Gozzi, and G. Balducci, J. Phys.: Condens. Matter **12**, 6971 (2000).
[9] N. Nagasako, A. Fukumoto, and K. Miwa, Phys. Rev. B **66**, 155106 (2002).
[10] S. Hong and C. L. Fu, Phys. Rev. B **66**, 094109 (2002).
[11] M. B. Moffett, A. E. Clark, M. Wun-Fogle, J. Linderberg, J. B. Teter, and E. A. Mclaughlin, J. Acoust. Soc. Am. **89**, 1448 (1991).
[12] H. Uchida, Y. Matsumura, H. Uchida, and H. Kaneko, J. Magn. Magn. Mater. **239**, 540 (2002).
[13] F. Chu, D. J. Thoma, P. G. Kotula, S. Gerstl, T. E. Mitchell, I. M. Anderson, and J. Bentley, Philos. Mag. A **77**, 941 (1998).
[14] F. Chu, D. J. Thoma, T. E. Mitchell, M. Sob, and C. L. Lin, Philos. Mag. B **77**, 121 (1998).
[15] C. T. Liu, J. H. Zhu, M. P. Brady, C. G. McKamey, and L. M. Pike, Intermetallics **8**, 1119 (2000).
[16] P. M. Robinson and M. B. Bever, in *Intermetallic Compound*, edited by J. H. Westrook (Wiley, New York, 1967), p. 38.
[17] J. H. Zhu, C. T. Liu, L. M. Pike, and P. K. Liaw, Intermetallics **10**, 579 (2002).
[18] A. Ormeci, F. Chu, J. M. Wills, T. E. Mitchell, R. C. Albers, D. J. Thoma, and S. P. Chen, Phys. Rev. B **54**, 12753 (1996).
[19] Y. Kubota, M. Takata, M. Sakata, T. Ohba, K. Kifune, and T. Tadaki, J. Phys.: Condens. Matter **12**, 1253 (2000).
[20] P. Rez, in *Transmission Electron Energy Loss Spectrometry in Materials Science*, edited by M. M. Disko, C. C. Ahn, and B. Fultz (Minerals and Materials Society, New Orleans, 1992), p. 107.
[21] R. F. Egerton, *EELS in the Electron Microscope* (Plenum, New York, 1986).
[22] D. A. Muller, T. Sorch, S. Moccio, F. H. Baumann, K. E. Lutterodt, and G. Timp, Nature (London) **399**, 758 (1999).
[23] G. A. Botton, G. Y. Guo, W. M. Temmerman, and C. J. Humphreys, Phys. Rev. B **54**, 1682 (1996).
[24] D. A. Muller, D. J. Singh, and J. Silcox, Phys. Rev. B **57**, 8181 (1998).
[25] P. L. Potapov, S. E. Kulkova, D. Schryvers, and J. Verbeeck, Phys. Rev. B **64**, 184110 (2001).
[26] K. Schwarz, P. Blaha, and G. K. H. Madsen, Comput. Phys. Commun. **126**, 71 (2002).
[27] J. P. Perdew, K. Burke, and M. Ernzerhof, Phys. Rev. Lett. **77**, 3865 (1996).
[28] P. E. Blöchl, O. Jepsen, and O. K. Anderson, Phys. Rev. B **49**, 16223 (1994).
[29] J. Sun and B. Jiang, Philos. Mag. (to be published).
[30] J. F. Lynch, J. R. Johnson, and R. C. Bowman, NATO Conference Series 6, 437 (1983).
[31] T. Nakamicmi, Y. Aoki, and M. Yamamoto, J. Phys. Soc. Jpn. **25**, 77 (1968).
[32] D. D. Vvedebsky, in *Unoccupied Electronic States: Fundamental of XANES, EELS, IPS and BIS*, Topics in Applied Physics Vol. 69, edited by J. C. Fuggle and J. E. Englishfield (Springer, Berlin, 1992).
[33] M. Nelhiebel, P.-H. Louf, P. Schattschneider, P. Blaha, K. Schwarz, and B. Jouffrey, Phys. Rev. B **59**, 12807 (1999).
[34] B. T. Thole and G. van der Laan, Phys. Rev. B **38**, 3158 (1988).
[35] R. F. Egerton and Z. L. Wang, Ultramicroscopy **32**, 137 (1990).
[36] R. D. Leapman, L. A. Grunes, and P. L. Fejes, Phys. Rev. B **26**, 614 (1982).
[37] P. E. Müller and J. W. Wilkins, Phys. Rev. B **29**, 4331 (1984).
[38] D. H. Pearson, B. Fultz, and C. C. Ahn, Appl. Phys. Lett. **53**, 1405 (1988).
[39] D. H. Pearson, C. C. Ahn, and B. Fultz, Phys. Rev. B **47**, 8471 (1993).
[40] R. D. Leapman, P. Rez, and D. F. Mayers, J. Chem. Phys. **72**, 1232 (1980).
[41] G. A. Botton and C. J. Humphreys, Micron **28**, 313 (1997).
[42] A. L. Ankudinov, A. I. Nesvizhskii, and J. J. Rehr, Phys. Rev. B **67**, 115120 (2003).
[43] M. Takata, Y. Kubota, and M. Sakata, Acta Crystallogr., Sect. A: Found. Crystallogr. **52**, 287 (1996).
[44] F. C. Frank and J. S. Kasper, Acta Crystallogr. **12**, 483 (1959).
[45] A. Hirata and Y. Koyama, Phys. Rev. B **67**, 144107 (2003).